

Conductive Imidazolium Side Chain Liquid Crystal Polyacrylates Prepared from Postpolymerization Functionalization

Caihong Wang, Yong Wu, Shuai Tan, Ting Liang, Xiaohui Yang

College of Chemical Engineering, Sichuan University, Chengdu 610065, China

Correspondence to: Y. Wu (E-mail: wuyong@scu.edu.cn)

ABSTRACT: Hydroxide and tetrafluoroborate salts of imidazolium polyacrylates have been prepared from postpolymerization functionalization of a brominated precursor containing mesogenic side chains followed by anion exchange. The ionic polyacrylates possessed molecular weights in the range $1.1\text{--}1.3 \times 10^4 \text{ g}\cdot\text{mol}^{-1}$. Differential scanning calorimetry measurements and polarizing optical microscope observation indicated that the resultant ionic polyacrylates exhibited smectic C and A liquid crystal phases over a temperature range of about 60°C . Electrochemical impedance spectroscopy measurements show that ionic conductivities of the hydroxide salt were much higher than those of the tetrafluoroborate salt for the imidazolium polyacrylates at the same temperature. The maximum ionic conductivity of the random hydroxide salt of imidazolium polyacrylate in the smectic A phase reached $4.45 \times 10^{-2} \text{ S}\cdot\text{cm}^{-1}$. The ionic polyacrylates were successfully aligned by mechanical shearing in the smectic A phase. Ionic conductivities of the sheared samples were more than 1 order of magnitude higher than those of the random samples in the solid state. © 2014 Wiley Periodicals, Inc. *J. Appl. Polym. Sci.* **2015**, *132*, 41564.

KEYWORDS: conducting polymers; ionic liquids; liquid crystals

Received 22 July 2014; accepted 26 September 2014

DOI: 10.1002/app.41564

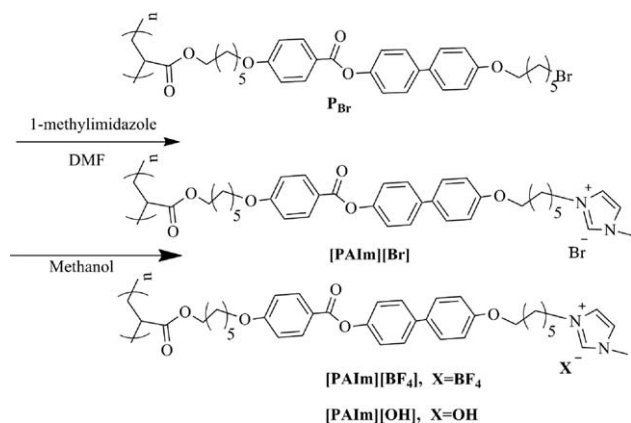
INTRODUCTION

Ionic liquid crystals are emerging as a new class of materials combining together the properties of ionic liquids and liquid crystals.¹ They have already found applications in ionic conduction, nanoparticle electrosynthesis, and energy-conversion.^{2–6} Imidazolium salts were widely used as ionic moieties because of their thermal stability, nonflammability, and high ionic conductivity.^{7,8} A few molecular designs have been explored for preparing imidazolium liquid crystals. The 1-alkyl-3-methylimidazolium and *N,N'*-dialkylimidazolium salts exhibited smectic phases owing to the amphiphilic structures.^{9,10} Attaching mesogens including biphenyl, phenyl benzoate, and azobenzene to substituted imidazolium salts also resulted in smectic liquid crystals.¹¹ Columnar and bicontinuous cubic phases were observed in *N*-methylimidazolium and 2-methyl-*N*-methylimidazolium salts containing triphenylene cores.¹²

Imidazolium ionic liquid crystal polymers are attractive because they combine the characteristics of low molecular weight liquid crystals with the mechanical properties of polymers. Kato et al. prepared columnar and smectic imidazolium polymers, in which linear or lamellar ionic pathways formed by virtue of mesophases.^{13,14} These ionic polymers were obtained by photopolymerization of aligned imidazolium liquid crystals having acrylate groups at the terminal sites. However, polymerization

of imidazolium liquid crystal monomers does not necessarily bring about a mesomorphic polymer. For example, polymers prepared from bromide salts of vinylimidazolium ionic liquids containing mesogenic coumarin and biphenyl were amorphous and did not show any mesophase.¹⁵

In this study, we demonstrate an alternative strategy to prepare imidazolium liquid crystal polymers. We have modified a brominated side chain liquid crystal polymer successfully with 2-hydroxyethanesulfonic acid sodium salt to obtain mesomorphic sulfonated polymers.^{16,17} In this report, hydroxide and tetrafluoroborate salts of imidazolium polyacrylates were prepared by postpolymerization functionalization of the same brominated precursor with 1-methyl-1*H*-imidazole. Fourier transform infrared (FT-IR) and ¹H nuclear magnetic resonance (¹H NMR) suggested complete functionalization of the precursor. The resultant ionic polymers exhibited smectic C and A phases over a broad temperature range. Temperature dependent ionic conductivities obtained by electrochemical impedance spectroscopy (EIS) measurements shows that ionic conductivities of the hydroxide salt were much higher than those of the tetrafluoroborate salt for the imidazolium polyacrylates at the same temperature. Ionic conductivities of the imidazolium liquid crystal polyacrylates were enhanced significantly after they were aligned by mechanical shearing in the smectic phase. The imidazolium



Scheme 1. Synthesis route of the mesomorphic imidazolium polyacrylates.

side chain liquid crystal polyacrylates prepared from postpolymerization functionalization have potential application in electrochemical devices such as alkaline solid fuel cells.

EXPERIMENTAL

The synthetic strategy of the imidazolium liquid crystal polyacrylates is shown in Scheme 1. Postpolymerization functionalization of the brominated mesomorphic precursor (P_{Br}) with 1-methyl-1H-imidazole gave bromide salt of imidazolium polyacrylate ($[\text{PAIm}][\text{Br}]$). The anion exchange reactions of $[\text{PAIm}][\text{Br}]$ with silver tetrafluoroborate and potassium hydroxide yielded tetrafluoroborate salt of imidazolium polyacrylate $[\text{PAIm}][\text{BF}_4]$ and hydroxide salt of imidazolium polyacrylate $[\text{PAIm}][\text{OH}]$, respectively.

Materials and Instrumentation

All commercially-available starting materials, reagents, and solvents were used as supplied and were obtained from TCI, Acros and Chengdu Changzheng. All reactions were performed using a dry nitrogen atmosphere.

^1H NMR spectra were measured on a Bruker AV II-400 spectrometer. FT-IR spectra were conducted on a NEXUS 670 FT-IR spectrometer. The molecular weights were determined on a gel permeation chromatography (GPC) with Tosoh HLC-8320 high-speed liquid chromatograph equipped with two TSK gel Super HM-H column (6×150 mm) at 70°C . Dimethyl fumarate (DMF) containing $0.05 \text{ mol}\cdot\text{L}^{-1}$ lithium bromide was used as a solvent at a flow rate of $0.3 \text{ mL}\cdot\text{min}^{-1}$. Differential scanning calorimetry (DSC) measurements were performed on a TA modulated Netzsch DSC 204 F1. Thermogravimetric analysis (TGA) were performed in a nitrogen atmosphere using a TA instrument Netzsch TGA 209C. The heating and cooling rates were $10^\circ\text{C}\cdot\text{min}^{-1}$. Cross-polarizing optical microscopies were captured by using a Weituo XPL-30TF polarizing optical microscope (POM) equipped with a WT-3000 hot-stage. X-ray diffraction (XRD) data was collected on a Philips X'Pert pro diffractometer using $\text{CuK}\alpha$ radiation at 40 kV and 40 mA. EIS was recorded on an electrochemical workstation consisted of an EG&G Princeton applied research potentiostat/galvanostat model 273A and PAR lock-in-amplifier model 5210 connected to a PC running electrochemical impedance software (Frequency range: $10 \text{ mHz}\sim 100 \text{ KHz}$, applied voltage: 10 mV). The cell for

EIS measurements consisted of a pair of indium tin oxide (ITO) electrodes. The distance (L) between the two electrodes was fixed by a perforated teflon spacer to be 0.014 cm . Before measurement, the sample was held in the hole ($A = 0.08 \text{ cm}^2$) of the spacer at isotropic temperature for several hours. After the cell was slowly cooled to room temperature, impedance spectra were recorded during a heating scan.

Synthesis of Bromide Salt of Imidazolium Polyacrylate ($[\text{PAIm}][\text{Br}]$)

The brominated precursor containing mesogenic side chains (P_{Br}) was prepared according to the procedure described previously.^{16,17} The molecular weight of P_{Br} was $1.1 \times 10^4 \text{ g}\cdot\text{mol}^{-1}$. A mixture of P_{Br} (3 g) and excess 1-methyl-1H-imidazole (2.08 g, 25.3 mmol) was stirred in DMF (10 ml) at 60°C for 72 h in a light-resistant container. The crude product was precipitated by adding 150 mL tetrahydrofuran (THF). The precipitate was then washed with methanol and the solution was concentrated *in vacuo* to give $[\text{PAIm}][\text{Br}]$ (2 g) in a yield of 67%. The ^1H NMR (400 MHz CDCl_3) δ (ppm): 10.85 (1H, $\text{N}=\text{CH}-\text{N}$), 8.14 (2H, Ar), 7.50 (4H, Ar), 7.15–7.13 (2H, $\text{N}-\text{CH}=\text{CH}-\text{N}$), 6.98 (6H, Ar), 4.36–4.18 (2H, CH_2-N), 4.06 (2H, OCH_2), 4.02 (4H, OCH_2), 3.78 (3H, $\text{N}-\text{CH}_3$), 1.75–0.6 (19H, CH_2); FT-IR (KBr): 3157, 3100, 2937, 2860, 1729, 1605, 1500, 1468, 1260, 1170, and 1074 cm^{-1} .

Synthesis of Tetrafluoroborate Salt of Imidazolium Polyacrylate ($[\text{PAIm}][\text{BF}_4]$)

A solution of silver tetrafluoroborate (0.75 g, 3.84 mmol) in methanol (20 mL) was added drop-wise to a solution of $[\text{PAIm}][\text{Br}]$ (2.0 g) in methanol with stirring at 0°C . The mixture was then stirred at room temperature in the dark for 24 h. An insoluble material was removed through a suction funnel and the solution was concentrated *in vacuo*. The residue was then dissolved in chloroform to remove inorganic salts and the solution was concentrated *in vacuo* to give $[\text{PAIm}][\text{BF}_4]$ (1.8 g) in a yield of 90%. The ^1H NMR (400 MHz CDCl_3) δ (ppm): 9.36 (1H, $\text{N}=\text{CH}-\text{N}$), 8.14 (2H, Ar), 7.48 (4H, Ar), 7.15–7.13 (2H, $\text{N}-\text{CH}=\text{CH}-\text{N}$), 6.96 (6H, Ar), 4.36–4.18 (2H, CH_2-N), 4.06 (2H, eOCH_2), 4.02 (4H, OCH_2), 3.78 (3H, $\text{N}-\text{CH}_3$), 1.75–0.6 (19H, CH_2); FT-IR (KBr): 3157, 3100, 2927, 2856, 1729, 1605, 1500, 1470, 1260, 1170, 1075, and 1035 cm^{-1} .

Synthesis of Hydroxide Salt of Imidazolium Polyacrylate ($[\text{PAIm}][\text{OH}]$)

A solution of potassium hydroxide (0.11 g, 1.92 mmol) in methanol (10 mL) was added drop-wise to a solution of $[\text{PAIm}][\text{Br}]$ (1.0 g) in methanol with stirring at 0°C . The mixture was stirred at room temperature in the dark for 24 h. An insoluble material was removed through a suction funnel and the solution was concentrated *in vacuo*. The residue was then dissolved in chloroform to remove inorganic salts and the solution was concentrated *in vacuo* to obtain $[\text{PAIm}][\text{OH}]$ (0.94g) in a yield of 94%. The ^1H NMR (400 MHz CDCl_3) δ (ppm): 8.90 (1H, $\text{N}=\text{CH}-\text{N}$), 8.04 (2H, Ar), 7.40 (4H, Ar), 7.15–7.13 (2H, $\text{N}-\text{CH}=\text{CH}-\text{N}$), 6.98 (6H, Ar), 4.36–4.18 (2H, CH_2-N), 4.02 (2H, OCH_2), 4.12 (4H, OCH_2), 3.88 (3H,

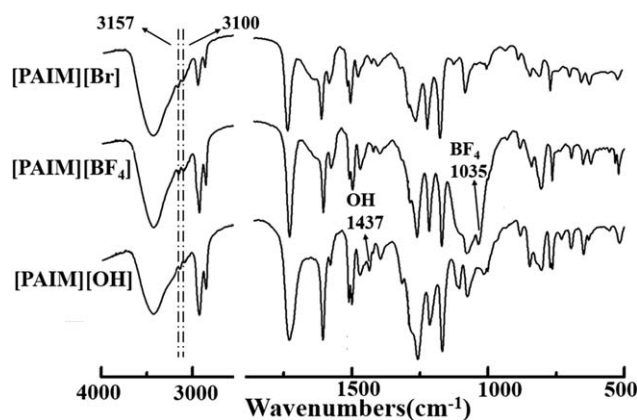


Figure 1. FT-IR spectra of [PAIm][Br], [PAIm][BF₄], and [PAIm][OH].

N—CH₃), 1.75–0.6(19H, CH₂); FT-IR (KBr)*v*: 3156, 3100, 2932, 2857, 1730, 1607, 1500, 1470, 1437, 1258, 1169, and 1076 cm⁻¹.

RESULTS AND DISCUSSION

Structural Characterization

The structures of the [PAIm][Br], [PAIm][BF₄], and [PAIm][OH] were well characterized. The FT-IR spectra of the polymers are shown in Figure 1 and the characteristic IR bands are listed in Table I. The bands at 3156 and 3100 cm⁻¹ were ascribed to C—H stretching of imidazolium rings. The presence of imidazolium ring indicated successful functionalization of the brominated precursor. The absorption band at 1035 cm⁻¹ in the spectrum of [PAIm][BF₄] was attributed to stretching vibration of tetrafluoroborate anions. The absorption band at 1437 cm⁻¹ in the spectrum of [PAIm][OH] was assigned to in plane bending vibration of hydroxide anions.

The ¹H NMR spectra of the imidazolium polymers are shown in Figure 2. The peaks at 4.36 and 4.18 ppm suggested the presence of imidazolium cation. Chemical shifts for N=CH—N were sensitive to anion type, which were observed at 10.85, 9.36, and 8.90 ppm in the spectra of [PAIm][Br], [PAIm][BF₄], and [PAIm][OH], respectively. These shifts agreed well with ¹H NMR spectra of imidazolium cations reported in literatures.^{18–20} The absence of shift at 3.44 ppm, which was ascribed to alkyl

Table I. Characteristic IR Bands in cm⁻¹ of [PAIm][BF₄] and [PAIm][OH]

Vibrational mode of functional groups	[PAIm][BF ₄]	[PAIm][OH]
Imidazolium ring C—H stretching	3157, 3100	3156, 3100
Alkyl C—H stretching	2927, 2856	2932, 2857
C=O stretching	1729	1730
Aromatic ring stretching	1607–1470	1607–1470
OH ⁻ bending	—	1437
CH ₂ twisting	1260	1258
C—C stretching	1170	1169
C—O—C stretching	1075	1076
BF ₄ ⁻ stretching	1035	—

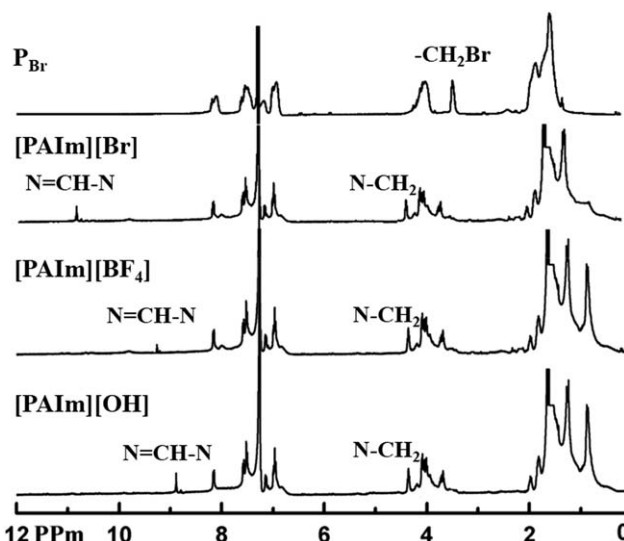


Figure 2. ¹H NMR spectra of [PAIm][Br], [PAIm][BF₄], and [PAIm][OH].

protons linked to the bromide groups of the precursor suggested the complete functionalization.

Mesophases of the Imidazolium Polyacrylates

DSC and TGA thermograms of the ionic polyacrylates are shown in Figure 3 and the 5% weight loss temperatures under a nitrogen atmosphere are listed in Table II. [PAIm][BF₄] had a higher thermal stability than [PAIm][OH]. [PAIm][OH] and [PAIm][BF₄] exhibited more than one decomposition step as other imidazolium ionic liquids did.²¹ The initial decomposition of [PAIm][BF₄] was assumed to be triggered by dealkylation of the cation via an S_N2 mechanism, whereas the decomposition of [PAIm][OH] was likely initiated by a ring opening reaction caused by the attack of hydroxide anion.^{22,23}

The DSC thermograms suggested that the imidazolium polyacrylates exhibited two mesophases during the heating scan. The phase types were assigned based on POM observation. In the

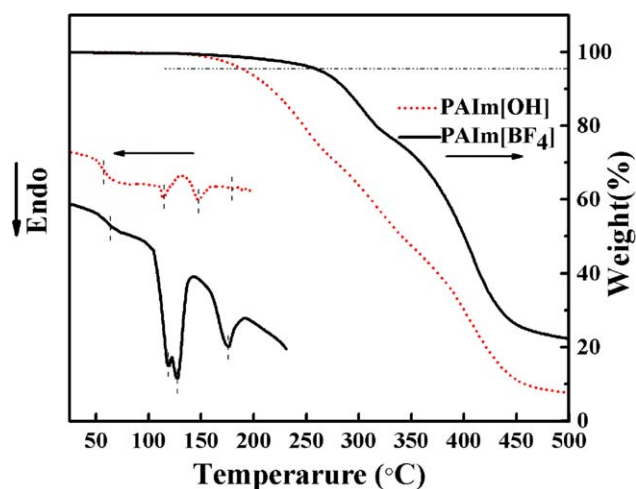


Figure 3. DSC/TGA thermograms of [PAIm][BF₄] and [PAIm][OH]. [Color figure can be viewed in the online issue, which is available at wileyonlinelibrary.com.]

Table II. Transition Temperatures and Associated Enthalpy Changes of [PAIm][BF₄] and [PAIm][OH]

Polymer	M_w (g·mol ⁻¹)	Phase transition temperature (°C) (enthalpy changes (J·g ⁻¹))	T_d (°C) ^a
[PAIm][BF ₄]	1.3×10^4	G 59 K 114 (- ^b) S _C 128 (- ^b) S _A 174 (5.6) I	273
[PAIm][OH]	1.1×10^4	G 55 K 88 (1.8) S _C 112 (2.4) S _A 146 (0.1) I	209

S_A, smectic A; S_C, smectic C; K, crystalline; G, glassy; I, isotropic.

^aTemperature of 5% weight loss.

^bValue is underivable because of the overlapping peaks.

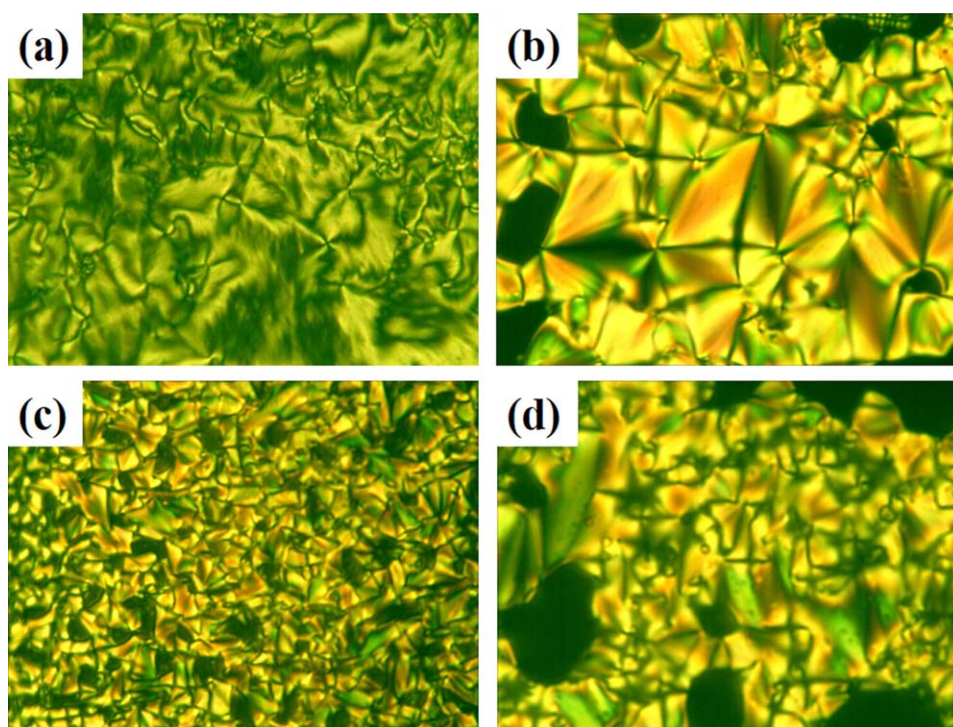


Figure 4. Polarized optical micrographs (600× magnification) of [PAIm][BF₄] at 120°C (a) and 135°C (b); [PAIm][OH] at 100°C (c), and [PAIm][OH] at 135°C (d). [Color figure can be viewed in the online issue, which is available at wileyonlinelibrary.com.]

case of [PAIm][BF₄], a broken focal conic texture was observed when the sample was heated to 114°C and smectic C phase was assigned. Upon further heated to 128°C, a characteristic focal conic texture suggested that smectic A phase developed. Bire-

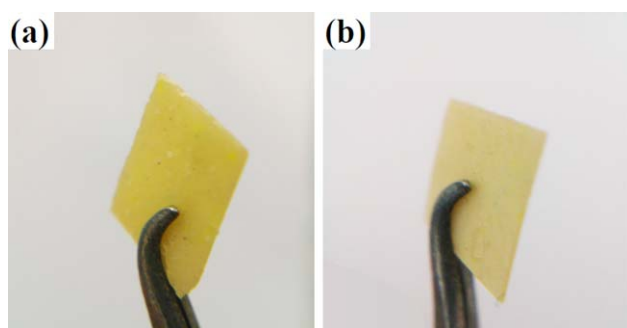


Figure 5. Photographs of [PAIm][BF₄] (a) and [PAIm][OH] (b) films. [Color figure can be viewed in the online issue, which is available at wileyonlinelibrary.com.]

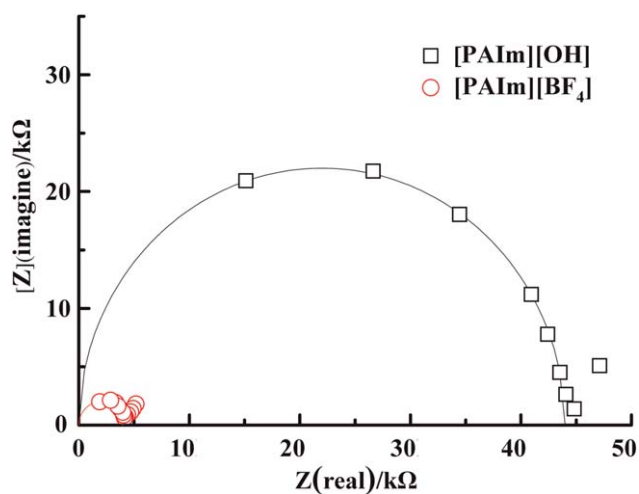


Figure 6. Impedance spectra for [PAIm][OH] at 40°C and [PAIm][BF₄] at 120°C.

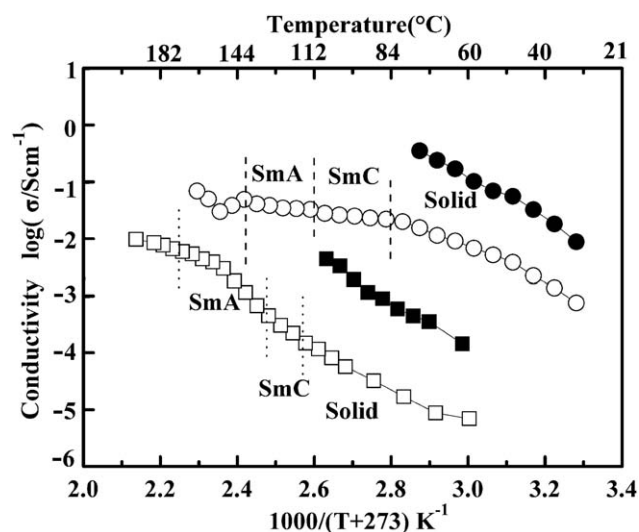


Figure 7. Temperature dependence of the ionic conductivity of the random [PAIm][BF₄] (□), random [PAIm][OH] (○), sheared [PAIm][BF₄] (■), and sheared [PAIm][OH] (●).

fringence disappeared as [PAIm][BF₄] became isotropic at 174°C. The characteristic textures observed for [PAIm][BF₄] and [PAIm][OH] are shown in Figure 4. XRD measurements had been performed to explore molecular arrangements in the mesophases. However, no clear small angle reflection was observed for the smectic phases formed by the imidazolium polyacrylates. Fully interleaved packing of side chains, as the smectic structure of side chain methylpolyacrylates suggested by

Cook et al.,²⁴ may account for the XRD patterns. The phase transition temperatures and corresponding enthalpy changes derived from the DSC thermograms are listed in Table II. Both [PAIm][BF₄] and [PAIm][OH] exhibited liquid crystal phases over a temperature range of about 60°C. Because protons of imidazolium ring and fluorine atoms of tetrafluoroborate anion may form hydrogen bonding,^{25,26} [PAIm][BF₄] had higher phase transition temperatures than [PAIm][OH].

Self-standing [PAIm][BF₄] and [PAIm][OH] films were obtained through melt-casting method. Anion type had little effect on the appearance of the casted imidazolium polyacrylates. As shown in Figure 5, both films were opaque and pale yellow.

Ionic Conductivities of the Imidazolium Polyacrylates

Temperature dependent impedance spectra for [PAIm][BF₄] and [PAIm][OH] were obtained by the EIS technique previously reported for measurements of ionic liquid crystals.^{27,28} Impedance responses were characterized by the semicircles at high frequencies, as shown in Figure 6. The resistance (R_b) was estimated from the intersection of the real axis (Z') and the semicircle of the impedance spectrum. The direct current polarization measurements suggested that the charge transport in the imidazolium polymers was predominant ionic conduction with a negligible contribution from electrons. The ionic conductivity σ was calculated using the following equation:

$$\sigma = \frac{L}{R_b A}$$

where L is the distance (cm) between electrodes and A is the sample area (cm²).

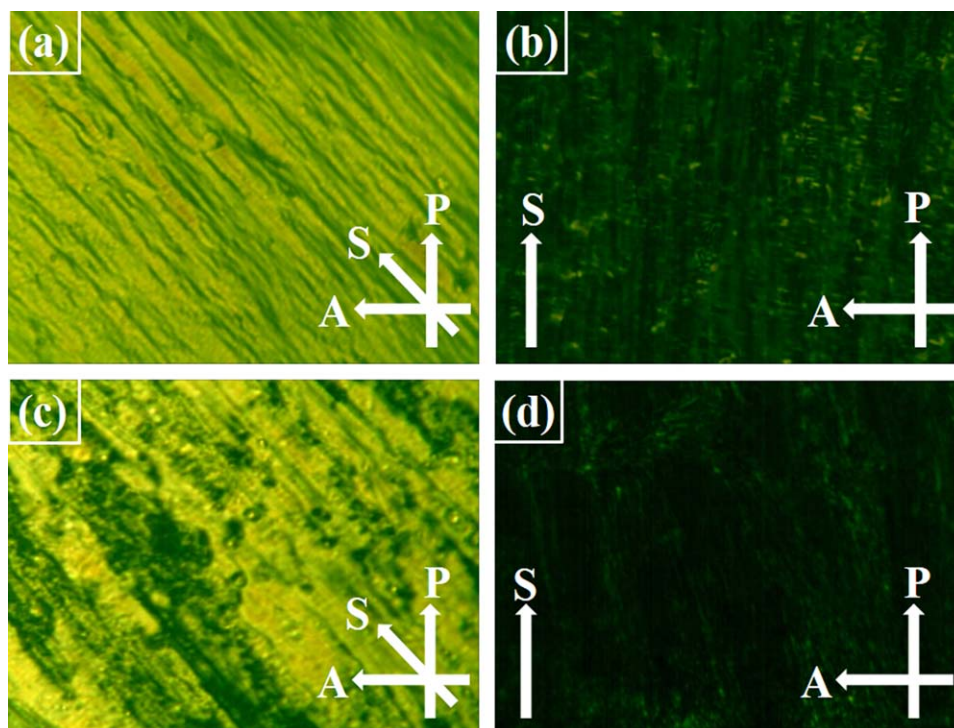


Figure 8. Polarized optical micrographs (600× magnification) of [PAIm][OH] sheared at 130°C (a), [PAIm][OH] sheared at 130°C with 45° deflection (b), [PAIm][BF₄] sheared at 155°C (c), and [PAIm][BF₄] sheared at 155°C with 45° deflection (d). Directions of A: analyzer; P: polarizer; S: shearing. [Color figure can be viewed in the online issue, which is available at wileyonlinelibrary.com.]

Conductivities of [PAIm][BF₄] and [PAIm][OH] increased with increase of temperature over the temperature range up to the isotropic point, as shown in Figure 7. In a specific phase, $\log \sigma$ versus $1/T$ approximately followed a straight line. This ionic conduction rule was also observed for nonmesomorphic side chain imidazolium polyacrylates.²⁹ However, the increase in the conductivity was slightly discontinuous at the phase transition temperatures for [PAIm][BF₄] and [PAIm][OH]. The fact suggested that phase type had effect on ionic conductivity. It was assumed that ionic conduction in imidazolium polymers depends on the mobility and nature of the corresponding anion and on glass transition temperature.³⁰ For the imidazolium liquid crystal polyacrylates, nature of the corresponding anion played an important role in the ionic conduction. Hydrogen bonding nets in [PAIm][BF₄] elevated energy barrier for ion transportation, whereas high diffusivity of hydroxide ions in [PAIm][OH] facilitated ion transportation.^{25,26,31} As a result, [PAIm][OH] exhibited superior ionic conductivities over [PAIm][BF₄]. Ionic conductivity of the random hydroxide salt of imidazolium polyacrylate was $7.6 \times 10^{-4} \text{ S}\cdot\text{cm}^{-1}$ at 30°C and reached $4.45 \times 10^{-2} \text{ S}\cdot\text{cm}^{-1}$ in the smectic A phase (144°C).

Side chain liquid crystal polymers exhibiting smectic phases can be macroscopically aligned under the effect of a mechanical field.^{32–34} The macroscopic alignments of the imidazolium polyacrylates were successfully achieved by mechanical shearing the random smectic samples in the sandwiched glasses. The sheared textures were retained upon rapidly cooling to room temperature for both [PAIm][BF₄] and [PAIm][OH]. Periodic change in brightness with the sample's rotation for polarizing microscopic observation suggested that long axes of most mesogenic side chains were parallel to the shear direction (Figure 8). When the rapidly cooled samples were reheated and held in the liquid crystal phases, the sheared textures collapsed gradually owing to molecular rearrangements.

To evaluate the effect of shearing alignment on ionic conduction in the solid state, EIS measurements were conducted using the same ITO electrodes. The conduction direction was perpendicular to the shear plane. The sheared sample exhibited much higher ionic conductivities than the corresponding random sample (Figure 7). The increase in conductivities had also been observed for uniformly aligned imidazolium liquid crystal polymers obtained by *in situ* photopolymerization.¹⁴ The enhanced conductivities in the sheared samples were ascribed to the increased ionic pathways formed in the regularly arranged molecules. Ionic conductivity of the sheared [PAIm][OH] reached $1.0 \times 10^{-2} \text{ S}\cdot\text{cm}^{-1}$ at 30°C, which was more than 1 order of magnitude higher than that of the random [PAIm][OH] at the same temperature.

CONCLUSIONS

Imidazolium salt terminated side chain polyacrylates containing hydroxide and tetrafluoroborate anions were prepared from postpolymerization functionalization of the mesomorphic brominated precursor. The ionic polyacrylates exhibited smectic C and A liquid crystal phases over a temperature range of

about 60°. Ionic conductivities of the hydroxide salt were much higher than those of the tetrafluoroborate salt for the imidazolium polyacrylates at the same temperature. The maximum ionic conductivity of the random hydroxide salt of imidazolium polyacrylate in the smectic A phase reached $4.45 \times 10^{-2} \text{ S}\cdot\text{cm}^{-1}$. The ionic liquid crystal polyacrylates were successfully aligned by mechanical shearing in the smectic A phase. Ionic conductivities of the sheared samples were more than 1 order of magnitude higher than those of the random samples in the solid state. The imidazolium side chain liquid crystal polyacrylates prepared from postpolymerization functionalization have potential application in electrochemical devices.

ACKNOWLEDGMENTS

This work was supported by the National Natural Science Foundation of China under the grant no. 20974068.

REFERENCES

1. Binnemans, K. *Chem. Rev.* **2005**, *105*, 4148.
2. Yoshio, M.; Mukai, T.; Ohno, H.; Kato, T. *J. Am. Chem. Soc.* **2004**, *126*, 994.
3. Shimura, H.; Yoshio, M.; Hoshino, K.; Mukai, T.; Ohno, H.; Kato, T. *J. Am. Chem. Soc.* **2008**, *130*, 1759.
4. Suisse, J. M.; Douce, L.; Bellemin-Lapponnaz, S.; Maise-François, A.; Welter, R.; Miyake, Y.; Shimizu, Y. *Eur. J. Inorg. Chem.* **2007**, *24*, 3899.
5. Dobbs, W.; Suisse, J. M.; Douce, L.; Welter, R. *Angew. Chem. Int. Ed.* **2006**, *45*, 4179.
6. Yamanaka, N.; Kawano, R.; Kubo, W.; Kitamura, T.; Wada, Y.; Watanabe, M.; Yanagida, S. *Chem. Commun.* **2005**, *6*, 740.
7. Welton, T. *Chem. Rev.* **1999**, *99*, 2071.
8. Dupont, J.; de Souza, R. F.; Suarez, P. A. Z. *Chem. Rev.* **2002**, *102*, 3667.
9. Holbrey, J. D.; Seddon, K. R. *J. Chem. Soc. Dalton Trans.* **1999**, *13*, 2133.
10. Lee, C. K.; Peng, H. H.; Lin, I. J. B. *Chem. Mater.* **2004**, *16*, 530.
11. Kouwer, P. H. J.; Swager, T. M. *J. Am. Chem. Soc.* **2007**, *129*, 14042.
12. Alam, M. A.; Motoyanagi, J.; Yamamoto, Y.; Fukushima, T.; Kim, J.; Kato, T.; Takata, M.; Saeki, A.; Seki, S.; Tagawa, S.; Aida, T. *J. Am. Chem. Soc.* **2009**, *131*, 17722.
13. Yoshio, M.; Kagata, T.; Hoshino, K.; Mukai, T.; Ohno, H.; Kato, T. *J. Am. Chem. Soc.* **2006**, *128*, 5570.
14. Hoshino, K.; Yoshio, M.; Mukai, T.; Kishimoto, K.; Ohno, H.; Kato, T. *J. Polym. Sci. Pol. Chem.* **2003**, *41*, 3486.
15. Jazkewitsch, O.; Ritter, H. *Macromol. Rapid Commun.* **2009**, *30*, 1554.
16. Tan, S.; Wang, C.; Wu, Y. *J. Mater. Chem. A.* **2013**, *1*, 1022.
17. Liang, T.; Tan, S.; Wang, C.; Wu, Y. *J. Appl. Polym. Sci.* **2014**, *131*, 40382.

18. Goossens, K.; Nockemann, P.; Driesen, K.; Goderis, B.; Görller-Walrand, C.; Van Hecke, K.; Van Meervelt, L.; Pouzet, E.; Binnemans, K.; Cardinaels, T. *Chem. Mater.* **2008**, *20*, 157.
19. Lin, S.; Ding, M.; Chang, C.; Lue, S. *Tetrahedron* **2004**, *60*, 9441.
20. Dobbs, W.; Douce, L.; Allouche, L.; Louati, A.; Malbosc, F.; Welter, R. *New J. Chem.* **2006**, *30*, 528.
21. Singh, M. P.; Singh, R. K.; Chandra, S. *Prog. Mater. Sci.* **2014**, *64*, 73.
22. Kroon, M. C.; Buijs, W.; Peters, C. J.; Witkamp, G. *Thermochim. Acta* **2007**, *465*, 40.
23. Ye, Y.; Elabd, Y. A. *Macromolecules* **2011**, *44*, 8494.
24. Cook, A. G.; Inkster, R. T.; Martinez-Felipe, A.; Ribes-Greus, A.; Hamley, I. W.; Imrie, C. T. *Eur. Polym. J.* **2012**, *48*, 821.
25. Tsuzuki, S.; Tokuda, H.; Mikami, M. *Phys. Chem. Chem. Phys.* **2007**, *9*, 4780.
26. Huang, J. F.; Chen, P. Y.; Sun, I. W.; Wang, S. P. *Inorg. Chim. Acta* **2001**, *320*, 7.
27. Dias, F. B.; Batty, S. V.; Ungar, G.; Voss, J. P.; Wright, P. V. *J. Chem. Soc. Faraday Trans.* **1996**, *92*, 2599.
28. Ohtake, T.; Ogasawara, M.; Ito-Akita, K.; Nishina, N.; Ujiie, S.; Ohno, H.; Kato, T. *Chem. Mater.* **2000**, *12*, 782.
29. Lee, J. H.; Lee, J. S.; Lee, J. W.; Hong, S. M.; Koo, C. M. *Eur. Polym. J.* **2013**, *49*, 1017.
30. Vygodskii, Y. S.; Shaplov, A. S.; Lozinskaya, E. I.; Lyssenko, K. A.; Golovanov, D. G.; Malyshkina, I. A.; Gavrilova, N. D.; Buchmeis, M. R. *Macromol. Chem. Phys.* **2008**, *209*, 40.
31. Ye, Y.; Sharick, S.; Davis, E. M.; Winey, K. I.; Elabd, Y. A. *Macro. Lett.* **2013**, *2*, 5575.
32. Zhao, Y.; Roche, P.; Yuan, G. *Macromolecules* **1996**, *29*, 4619.
33. Geng, J.; Zhao, X.; Zhou, E.; Li, G.; Lamb, J. W. Y.; Tang, B. *Z. Polymer* **2003**, *44*, 8095.
34. Wiberg, G.; Skytt, M. L.; Gedde, U. W. *Polym. Commun.* **1998**, *39*, 2983.